

Notes

Direct Visualization of Vesicle–Bilayer Complexes by Atomic Force Microscopy

Sanjay Kumar[†] and Jan H. Hoh^{*,†,‡}

Department of Physiology, Johns Hopkins University School of Medicine, Baltimore, Maryland 21205, and Department of Chemical Engineering, Johns Hopkins University, Baltimore, Maryland 21218

Received March 30, 2000. In Final Form: July 10, 2000

Introduction

Interactions between phospholipid vesicles and bilayers play a central role in cell physiology, enabling secretion, signaling, and intracellular transport. In many instances these processes require fusion between membranes. Considerable attention has been paid to acquiring the structural details of proteins that mediate fusion;¹ however, less is known about the structure and organization of lipids during this process. In addition, the interaction between lipids and proteins is known to be important for fusion. Evidence for this comes from the fact that when fusogenic proteins are reconstituted into lipid bilayers, their activities are often a sensitive function of lipid type (reviewed in ref 2). Substantial evidence also implicates membrane cholesterol content in the ability of some enveloped viruses to fuse with and enter liposomes.^{3–5} Because of this, the physical mechanisms of membrane fusion in reconstituted lipid systems have received intense study with a variety of physical methodologies that includes fluorescence spectroscopy and microscopy,⁶ light scattering,⁷ and the surface forces apparatus.⁸ These studies have revealed that membrane fusion propensity depends on several parameters including fluidity, lysis tension, and bending modulus and have produced a wealth of quantitative data on the mechanical properties of bilayers formed from different lipid compositions.

The atomic force microscope (AFM) is particularly well-suited to the characterization of reconstituted complexes of biological macromolecules because of its ability to operate under buffer, in real time, and at the nanometer length scale. Thus, much effort has been made to use AFM

to study lipid vesicles, planar bilayers, and other self-assembled lipid microstructures. Similarly, AFM would be an attractive tool with which to study structural intermediates in membrane fusion. Several investigators have presented AFM images of both purified synaptic vesicles and reconstituted phospholipid vesicles on solid substrates. The former studies^{9–11} have lent valuable insight into the mechanical properties of synaptic vesicles as well as how those properties change in the presence of biochemical effectors. The latter studies either have used receptor–ligand interactions to tether the vesicles to substrates such as gold¹² and mica¹³ or have focused on the kinetics and mechanisms of formation of supported bilayers from phospholipid vesicles.^{14,15} These studies have helped elucidate the various stages of membrane assembly. Nonetheless, definitive visualization of individual vesicles has been limited. Presumably, this is due in part to vesicle deformation during scanning and the presence of artifactual contributions from the AFM tip. Even less is known from AFM about the association of vesicles with a planar bilayer, including structural details of the processes of adsorption, wetting, and fusion. The same is true of vesicle–vesicle interactions; while aggregates of small unilamellar vesicles (SUVs) are well within the limits of AFM's spatial resolution, freeze-fracture electron microscopy remains the most widely used method for directly visualizing interactions between SUVs. Obtaining high-resolution images of vesicles in contact with each other and with planar membranes would serve as an important first step toward introducing AFM to the study of membrane fusion intermediates. Recent light microscopic studies with giant vesicles⁶ suggest that membrane fusion in vitro can proceed through an orderly sequence of adsorption, adhesion, wetting, and merger, any or all of which might be directly captured by the AFM.

In this report, we present AFM images of vesicle–bilayer complexes formed by adsorbing SUVs onto mica to form a continuous membrane and allowing excess vesicles to settle onto the membrane. We use depth measurements to show that we can successfully form a continuous supported membrane, and we present mechanical and structural evidence that the adsorbed structures truly are individual lipid vesicles. We also show that the morphology of the adsorbed structures is a function of lipid composition.

Materials and Methods

Preparation of Vesicle Suspensions. DPPC and cholesterol were obtained from Avanti Polar Lipids (Alabaster, AL) and used without further purification. Lipids were stored as both dry powders and stock solutions in chloroform at –20 °C. At the time

* Address correspondence to: Jan H. Hoh, Department of Physiology, Johns Hopkins University School of Medicine, 725 N. Wolfe Street, Baltimore, MD 21205. Phone: 410-614-3795. FAX: 410-614-3797. E-mail: jhoh@jhmi.edu.

(1) Hughson, F. M. *Curr. Opin. Struct. Biol.* **1995**, *5*, 507–513.

(2) Chernomordik, L. V.; Zimmerberg, J. *Curr. Opin. Struct. Biol.* **1995**, *5*, 541–547.

(3) Smit, J. M.; Bittman, R.; Wilschut, J. *J. Virol.* **1999**, *73*, 8476–8484.

(4) Bernardes, C.; Antonio, A.; de Lima, M. C. P.; Valdeira, M. L. *Biochim. Biophys. Acta* **1998**, *1393*, 19–25.

(5) Kanaseki, T.; Kawasaki, K.; Murata, M.; Ikeuchi, Y.; Ohnishi, S. *J. Cell Biol.* **1997**, *137*, 1041–1056.

(6) Pantazatos, D. P.; MacDonald, R. C. *J. Membr. Biol.* **1999**, *170*, 27–38.

(7) Asgharian, N.; Schelly, Z. A. *Biochim. Biophys. Acta* **1999**, *1418*, 295–306.

(8) Wong, J. Y.; Park, C. K.; Seitz, M.; Israelachvili, J. *Biophys. J.* **1999**, *77*, 1458–1468.

(9) Parpura, V.; Doyle, R. T.; Basarsky, T. A.; Henderson, E.; Haydon, P. G. *Neuroimage* **1995**, *2*, 3–7.

(10) Garcia, R. A.; Laney, D. E.; Parsons, S. M.; Hansma, H. G. *J. Neurosci. Res.* **1998**, *52*, 350–355.

(11) Laney, D. E.; Garcia, R. A.; Parsons, S. M.; Hansma, H. G. *Biophys. J.* **1997**, *72*, 806–813.

(12) Shibata-Seki, T.; Masai, J.; Tagawa, T.; Sorin, T.; Kondo, S. *Thin Solid Films* **1996**, *273*, 297–303.

(13) Pignataro, B.; Steinem, C.; Galla, H.-J.; Fuchs, H.; Janshoff, A. *Biophys. J.* **2000**, *78*, 487–498.

(14) Egawa, H.; Furusawa, K. *Langmuir* **1999**, *15*, 1660–1666.

(15) Reviakine, I.; Brisson, A. *Langmuir* **2000**, *16*, 1806–1815.

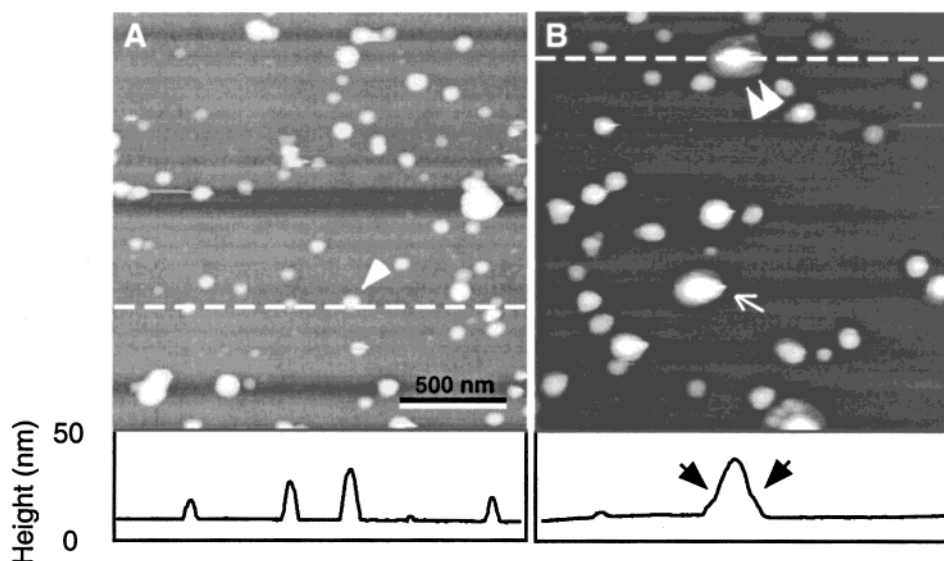


Figure 1. Height images and topographic profiles of vesicle-bilayer complexes made from 1:1 molar mixtures of DPPC and cholesterol. The dark background is the bilayer, and the lighter areas are material adsorbed onto the bilayer. Topographic profiles across several domelike structures (A, single solid arrow) and saucer-shaped structures (B, double solid arrows) are shown beneath the images. The arrows in the profile under (B) note the edges of a central protrusion observed for a typical saucer. The top portions of some vesicles are labile to AFM imaging, as indicated by streaks that emerge along the scanning direction from one side of the vesicle (open arrow). Both images are of equal size.

of sample preparation, 1.0 mg of total lipid was dried from stock solution for 1–2 h under a gentle stream of ultrahigh purity nitrogen followed by treatment with house vacuum over desiccant for 2–6 h. In some cases, the lipid was weighed directly as dry powder, with no discernible differences in results. The dry lipid was then resuspended in 1 mL of 20 mM NaCl buffer and sonicated under nitrogen in a Fisher ultrasonic cleaner until clear (usually 30–60 min). This suspension was then centrifuged at 16000*g* for 30 min to remove any large aggregates or contaminants.

Formation of Vesicle-Bilayer Complexes. We prepared our samples using a method based on the vesicle adsorption technique.^{16,17} Briefly, following centrifugation, 50 μ L of supernatant was pipetted onto a freshly cleaved mica substrate (grade V1 or V2, Asheville-Schoonmaker Mica Co., Newport News, VA) mounted onto a magnetic metal disk (Ted Pella, Redding, CA). The drop was confined by a homemade silicone O-ring affixed by a minimal amount of vacuum grease. To rule out artifacts of contamination, some samples were made without the O-ring or grease, with no detectable differences in results. After allowing the vesicles to adsorb at room temperature for 30 min, 100 μ L of excess buffer was added. Samples were then stored at 4 °C until imaging. Great care was taken to keep the sample continuously under buffer up to and during AFM imaging, and samples were discarded if allowed to dry prior to imaging.

Atomic Force Microscopy. Images and force measurements were obtained with a Multimode AFM with a Nanoscope III or IIIa controller (Digital Instruments, Santa Barbara, CA), using a glass fluid cell. All measurements were made with Olympus silicon nitride cantilevers (OMCL-TR400PSA, purchased from Digital Instruments) with lengths of 200 μ m and nominal spring constants of 0.02 N/m. Prior to imaging, the microscope, sample, and cantilever were allowed to equilibrate at room temperature for at least 1 h. All images were collected in contact mode. To produce elasticity maps, force volumes were obtained using the Nanoscope III software, and individual force curves were subsequently converted to plots of force versus distance-to-hard-contact.¹⁸ The curves were then analyzed with in-house software to obtain relative elasticity maps using the force integration to

equal limits (FIEL) method.¹⁹ Force volumes were collected in relative trigger mode; isoforce surfaces were constructed by mapping the piezo position at each point of relative trigger on the surface.

Results and Discussion

We first adsorbed DPPC-cholesterol (1:1 molar) SUVs onto mica to form a supported bilayer and allowed excess vesicles to settle to the membrane to form vesicle-bilayer complexes. This results in a surface covered by a high density of domelike protrusions that emerge 10–50 nm from the supported bilayer (Figure 1A). These domelike structures coexist with saucer-like structures, so-called because they resemble saucers resting face down on a flat surface, in which the central portion of the structure appears raised and rounded relative to its periphery (Figure 1B). A topographic profile along such a structure demonstrates that the height difference between periphery and center is approximately 10–20 nm. The characteristic feature of a saucer is a central protrusion that is of greater height than the edges. Underneath these vesicular structures is a flat, defect-free surface. A simple interpretation of these images is that the flat surface is a continuous lipid bilayer and the dome- and saucer-shaped structures are vesicles that have stably adsorbed to and wet the membrane. Some of the structures seen here are smaller in height than 20 nm, which is below the typical size range of sonicated vesicles. The reduction in apparent height may be explained by vesicle deformation due to wetting of the bilayer and compressive forces from the AFM tip.¹³ Another possibility is that the smallest structures in the image are nonvesicular structures such as cholesterol micelles. While this may indeed account for some of the smallest structures, we found these adsorbates to be present at significant numbers even at cholesterol mole fractions below 0.1.

To demonstrate that the surface underlying the adsorbed vesicles is a lipid bilayer, we scanned a 1 μ m \times 1

(16) Brian, A. A.; McConnell, H. M. *Proc. Natl. Acad. Sci. U.S.A.* **1984**, *81*, 6159–6163.

(17) Fang, Y.; Yang, J. *Biochim. Biophys. Acta* **1997**, *1324*, 309–319.

(18) Butt, H. J.; Jaschke, M.; Ducker, W. *Bioelectrochem. Bioenerg.* **1995**, *38*, 191–201.

(19) A-Hassan, E.; Heinz, W. F.; Antonik, M. D.; D'Costa, N. P.; Nageswaran, S.; Schoonenberger, C. A.; Hoh, J. H. *Biophys. J.* **1998**, *74*, 1564–1578.

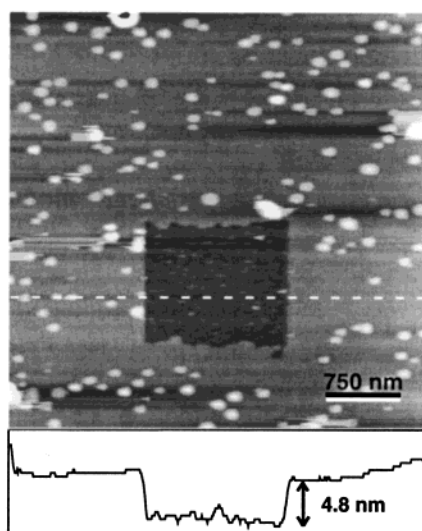


Figure 2. Thickness of DPPC-cholesterol bilayer demonstrated by AFM manipulation and imaging. Prior to obtaining this height image at minimal scanning forces, the central $1\ \mu\text{m} \times 1\ \mu\text{m}$ area was scanned at high imaging forces ($> 50\ \text{nN}$) and scan rate ($> 20\ \text{Hz}$) for 10 min, thereby scraping through to the underlying substrate. The topographic profile along the line drawn in the image is shown below. The height difference between the bilayer surface and the mica surface is approximately 4.8 nm, consistent with the expected thickness of a phospholipid bilayer.

μm region of a sample with a very high force (normal to the surface) to scrape through to the mica substrate and measure the bilayer thickness (Figure 2). The height difference between the lipid surface and the underlying mica substrate is approximately 4.8 nm, around the expected thickness of a phospholipid membrane.²⁰ This thickness is also consistent with values measured in solution with cholesterol-DPPC lamellae by X-ray diffraction.²¹

The adsorbed particles seen in Figure 1 are around the expected size and shape of individual lipid vesicles complexed with the bilayer. However, they are also of the same approximate dimensions and shape as the AFM tip itself. This raises the possibility that the vesicular structures may not be vesicles at all but rather convolutions of the AFM tip scanning objects with smaller radii of curvature than itself (e.g., contaminants, surface heterogeneities).²² Hence, tests that go beyond simple recognition of size and shape are needed to demonstrate that these are actually vesicles. One such test exploits the ability of the AFM to make indentation measurements. True vesicles are expected to be far more soft and compliant than the underlying membrane, which is mechanically tightly coupled to the rigid mica substrate. Therefore, we performed micromechanical mapping on the surface by force volume imaging.²³ An isoforce image constructed from a force volume of a 1:1 DPPC/cholesterol surface is shown in Figure 3A. The light-colored areas are low-resolution images of the adsorbates. An elasticity map was produced using the FIEL method (Figure 3B). The areas of low elasticity correspond in general to the positions of the adsorbates in Figure 3A. This difference in elasticity is more directly seen in the individual force curves collected

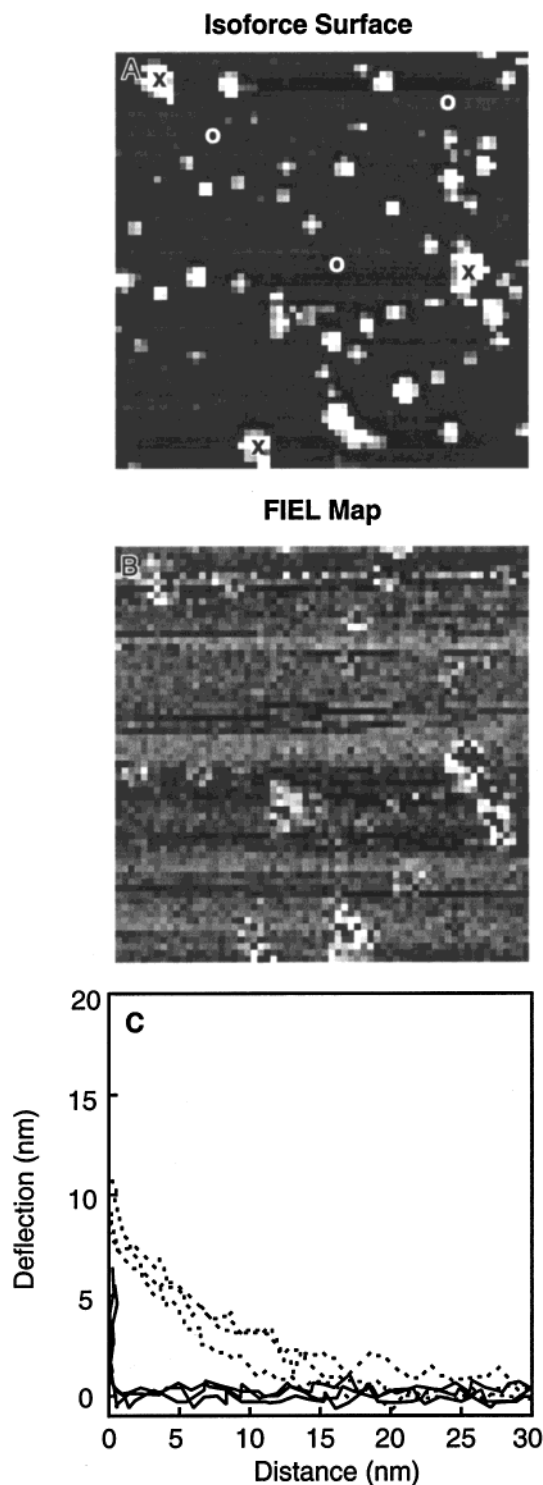


Figure 3. Elasticity measurements of adsorbed vesicles from force volumes. (A) A low force isoforce surface calculated from an array of 64×64 force curves collected over a $3\ \mu\text{m} \times 3\ \mu\text{m}$ area. The underlying bilayer appears as a dark background and adsorbed material appears as light regions. The tip-sample approach portions of these curves were integrated to determine relative elasticities,²³ resulting in the elasticity map shown in (B). Here, lighter colored regions correspond to softer (lower elasticity) regions of the sample. (C) Three force-distance curves each taken over bilayer regions (solid lines) and over adsorbates (dashed lines). The specific locations from which these force curves were taken are marked in (A) with either an \times (adsorbate) or an \circ (bilayer). Note that these curves have been shifted from cantilever deflection vs piezo position to deflection vs distance.¹⁸ A positive cantilever deflection prior to zero distance indicates sample deformation.

(20) Marsh, D. *Handbook of Lipid Bilayers*; CRC Press: Boca Raton, FL, 1990.

(21) Lemmich, J.; Mortensen, K.; Ipsen, J. H.; Honger, T.; Bauer, R.; Mouritsen, O. G. *Eur. Biophys. J. Biophys. Lett.* **1997**, *25*, 293–304.

(22) Hansma, H. G.; Hoh, J. H. *Annu. Rev. Biophys. Biomol. Struct.* **1994**, *23*, 115–139.

(23) Heinz, W. F.; Hoh, J. H. *Trends Biotechnol.* **1999**, *17*, 143–150.

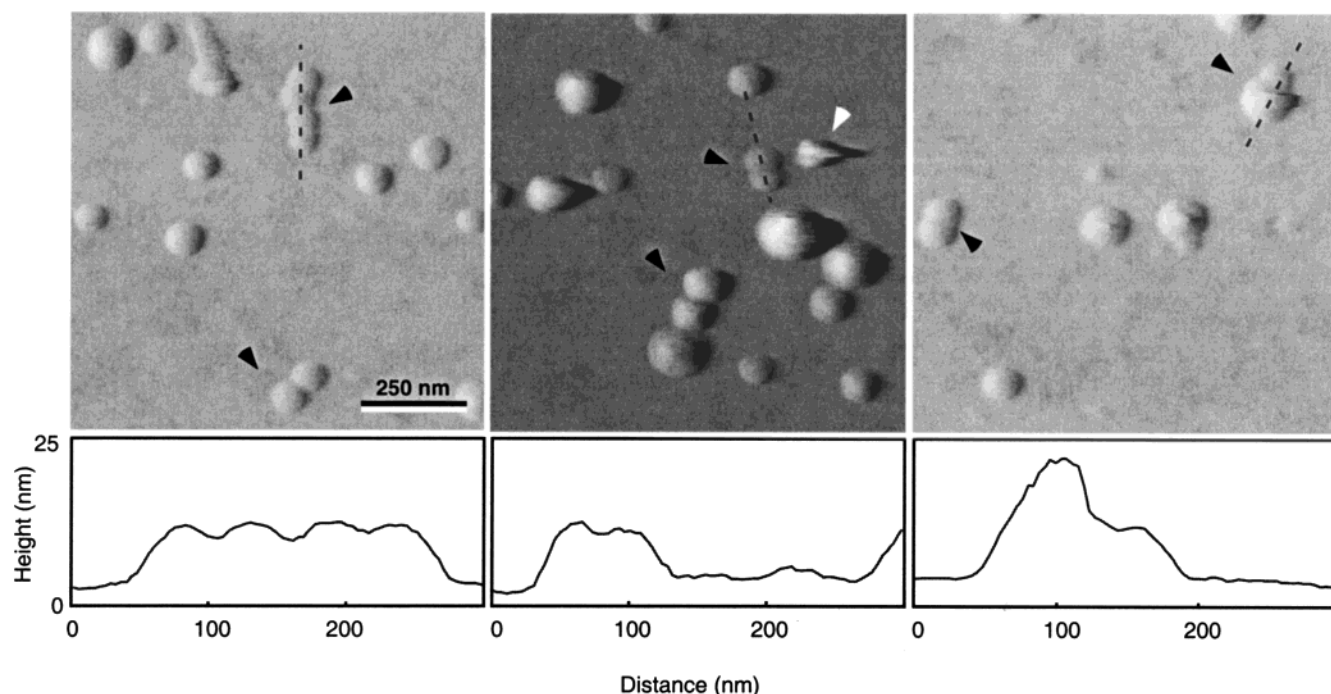


Figure 4. AFM images of vesicular structures in adhesive contact. Deflection images are shown of three examples of adjacent vesicles that have come into a flat interfacial contact (black arrows). All three images are of equal size. Height profiles taken along the dashed lines are shown beneath the images (note that the images are from the deflection signal whereas the profiles come from the corresponding topographic images which are not shown here). The middle image shows an example of where the AFM tip has either smeared away a piece of a vesicle or dragged it along the surface (white arrow). Again, dome- and saucer-like structures are shown coexisting on the bilayer.

on the flat part of the membrane and on the adsorbates (Figure 3C). There is essentially no deformation over the bilayer until 1–2 nm before hard contact. This small region of deformation may be due to the intrinsic elasticity of the bilayer itself. In contrast, there is a prolonged deformation region of at least 15 nm over a typical vesicle. Therefore, the adsorbed structures are far more compliant than the supported bilayer. The fact that the z -distance over which the vesicles are elastically deformed is around the same size as the vesicles themselves suggests that the vesicles are soft over their entire height. In addition to excluding a tip-shaped artifact, this softness also makes it unlikely that the adsorbates are particulate contaminants in the buffer. Finally, this deformability is consistent with both elasticity maps of cholinergic synaptic vesicles¹¹ and indentation measurements on biotinylated phospholipid vesicles bound to avidin-coated surfaces.¹³

A second test of whether these structures are truly vesicles comes from images of adjacent vesicles. Figure 4 shows three such examples. In all cases, the vesicular structures appear to come to a flat, mutually deforming interfacial contact. This type of interface is characteristic of two adherent vesicles and was observed by freeze-fracture electron microscopy of egg-phosphatidylcholine SUVs²⁴ and light microscopy of giant unilamellar vesicles.⁶ An additional feature of these adsorbates, as with the adsorbates shown in Figure 1, is that the highest points are soft and somewhat labile to AFM imaging resulting in streaks. These streaks suggest that the adsorbates are far softer or more mobile than the underlying bilayer, a finding consistent with the interpretation that they are bound vesicles. Indeed, we found that even at modestly high scanning forces, the adsorbates were readily dislodged from the surface. This is in contrast to the underlying bilayer, which at high cholesterol content proved quite resistant to tip-induced abrasion from the mica surface. To our knowledge, these are the first reported AFM images

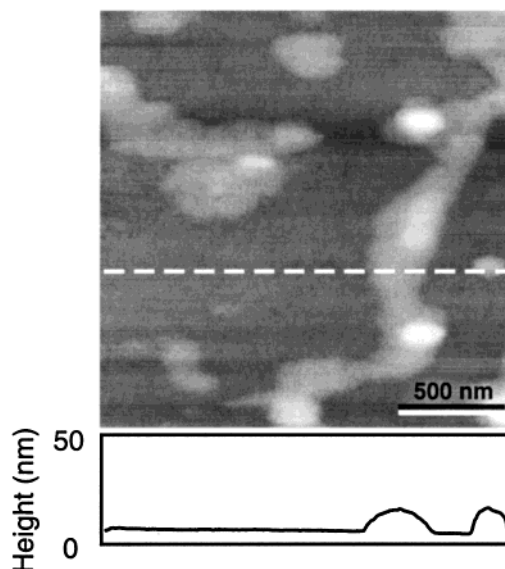


Figure 5. AFM image and topographic profile of vesicle–bilayer complexes formed from pure DPPC.

of coadsorbed lipid vesicles showing a flat contact interface and contact angle.

Finally, using the same method, we attempted to create vesicle–bilayer complexes with SUVs made of pure DPPC (Figure 5). In contrast to Figure 1, the surface is no longer covered by bound vesicles; instead, larger aggregates are found atop the first bilayer. These larger aggregates may be partial formation of a second bilayer or may result from multilamellar structures settling on the bilayer. The absence of individual vesicles for pure DPPC is consistent with a previous AFM report of multilayer formation by DPPC on mica.²⁵ Why cholesterol appears to stabilize the bound vesicles and prevent multilayering is likely a result

of the changes cholesterol is known to confer on phospholipid bilayers. These changes are well documented from micropipet aspiration studies and include increases in toughness, fluidity, bending and area expansion moduli, and lysis tension.²⁶ Interestingly, fluorescence spectroscopic studies of vesicle-vesicle fusion in vitro indicate that cholesterol has a biphasic effect on the ability of distearoylphosphatidylcholine vesicles to fuse with mixed phospholipid vesicles: total fusion increases at mole fractions less than 0.1 and then falls markedly up to 0.45.²⁷ Thus, one explanation for the unusual stability of bilayer-associated vesicles seen with our system may be the reduced fusion propensity of cholesterol-rich vesicles coupled with their increased mechanical rigidity. Answering this question conclusively will require detailed study of the effect of cholesterol content on the morphology and mechanical properties of the vesicle-bilayer complexes.

When DPPC-cholesterol SUVs were used to form the complexes, we repeatedly observed two distinct vesicular structures (dome shaped and saucer shaped). One interpretation is that the two structures are simply different types of stable intermediates that form when a vesicle wets or partially fuses with a bilayer. Whether this is a consequence of heterogeneities in vesicle size, lipid composition, or some other parameter is unclear. A second interpretation of the saucer-like structures relates to lamellarity. The saucer-like morphology may result from the adsorption and spreading of a multilamellar vesicle onto the surface; as the inner shells of the multilamellar structure wet the surface during adsorption, some com-

bination of surface tension and steric confinement by the outer shells arrests spreading. In this model, the edges of the saucer come from the outermost shells wetting the bilayer. Because sonication followed by centrifugation is generally thought to yield predominantly unilamellar structures, the high fraction of saucers is somewhat surprising. One possibility is that the few multilamellar structures that do remain adsorb more stably to the membrane surface than unilamellar structures. A third interpretation is that these structures are two vesicles stacked atop one another on the supported bilayer. If this was the case, however, one would expect that AFM scanning would frequently dislodge the topmost vesicle, leaving the bottom one intact. We have not observed this phenomenon in practice; instead, when scanning forces are sufficient to dislodge the saucer, the entire complex is removed, leaving only the underlying bilayer behind. Moreover, the central protrusion in a saucer is always quite centrally located; there is no a priori reason to expect that a second vesicle would always settle in such a centered fashion atop a first.

Because AFM allows the simultaneous acquisition of structural and mechanical data under aqueous conditions, the results presented here suggest the framework for a system with which interactions between vesicles and bilayers as well as early intermediates in membrane fusion may be probed at very high spatial and energetic resolution. This may permit the observation of vesicle adsorption, spreading, and fusion under aqueous conditions, in real time, and in response to soluble factors.

Acknowledgment. S.K. was supported in part by a Medical Scientist Training Program Fellowship from the National Institutes of Health.

LA000476W

(24) Bailey, S. M.; Chiruvolu, S.; Israelachvili, J. N.; Zasadzinski, J. A. N. *Langmuir* **1990**, *6*, 1326-1329.

(25) Fang, Y.; Yang, J. *J. Phys. Chem.* **1996**, *100*, 15614-15619.

(26) Needham, D.; Nunn, R. S. *Biophys. J* **1990**, *58*, 997-1009.

(27) Bailey, A. L.; Cullis, P. R. *Biochemistry* **1997**, *36*, 1628-1634.